

Fluorescent Molecular Rotors Based on the BODIPY Motif: Effect of Remote Substituents

*Effat Bahaidarah,^a Anthony Harriman,^{*a} Patrycja Stachelek,^a Sandra Rihn,^b Elodie Heyer,^b and Raymond Ziessel^b*

Supporting Information

^(a)Molecular Photonics Laboratory, School of Chemistry, Bedson Building, Newcastle University, Newcastle upon Tyne, NE1 7RU, United Kingdom and ^(b)Laboratoire de Chimie Organique et de Spectroscopies Avancées (ICPEES-LCOSA), UMR 7515 CNRS, 25 rue Becquerel, 67087 Strasbourg Cedex 2, France.

Table of Contents

Table S1. Photophysical properties in dichloromethane	S2
Tables S2-S6. Cartesian coordinates for the energy-minimized structures	S3
Table S7. Effect of temperature on the nonradiative rate constant	S10
Figure S1. Absorption, emission and excitation spectra for ROBOD and BOD	S11
Figure S2 Absorption, emission and excitation spectra for PHEN1, PHEN2 and CORE	S12
Figure S3 Effect of temperature on emission quantum yields	S14
Figure S4 Effect of temperature on emission spectrum of PHEN2	S15
Figure S5 Dihedral angle vs energy for PHEN1	S16
Figure S6 Kohn-Sham representations of HOMO and LUMO	S17
Figure S7 Energy-minimized geometries	S19
Experimental details	S25
References	S26

Table S1. Summary of the photophysical properties recorded for the target compounds in CH₂Cl₂ at 20 °C.

Property	ROBO	BOD	PHEN1	PHEN2	CORE
$\lambda_{\text{MAX}} / \text{nm}$	502	525	531	559	547
$\epsilon_{\text{MAX}} / \text{M}^{-1}\text{cm}^{-1}$	71,000	74,000	59,100	62,235	62,100
$\lambda_{\text{FLU}} / \text{nm}$	528	544	557	597	582
SS / cm ⁻¹	980	665	880	1,140	1,100
Φ_{F}	0.021	0.77	0.010	0.24	0.87
$\tau_{\text{S}} / \text{ns}$	0.16	5.4	0.07	2.06	6.4
$k_{\text{RAD}} / 10^8 \text{ s}^{-1}$	1.31	1.43	1.43	1.16	1.36
$k_{\text{NR}} / 10^8 \text{ s}^{-1}$	61	0.43	141	3.7	0.20

Table S2. Cartesian coordinates for the energy-minimized structure computed for ROBOD.

1	F	0.00000000	0.00000000	0.00000000
2	B	1.34650430	0.00000000	0.00000000
3	N	1.92517201	1.54095207	0.00000000
4	C	1.63589047	2.51296118	-0.93028897
5	C	2.32607996	3.73531058	-0.56524957
6	C	3.03522730	3.46733445	0.60941029
7	C	2.77552869	2.08603808	0.94760006
8	C	3.26793204	1.30882879	2.11918166
9	C	4.15111451	1.97501910	3.06040252
10	C	3.87994511	1.93591110	4.43600445
11	C	4.73321917	2.56350855	5.34062328
12	C	5.87357835	3.23744818	4.89119303
13	C	6.77310855	3.91702996	5.85141807
14	C	6.14682486	3.27404136	3.51815120
15	C	5.29339870	2.65427071	2.61036947
16	F	1.75167684	-0.65779598	-1.10295281
17	N	1.95479642	-0.64389872	1.34932714
18	C	2.84181174	0.02749982	2.25792585
19	C	3.17096764	-0.95081185	3.31748233
20	C	2.49582908	-2.12253466	3.02166906
21	C	1.75509689	-1.90230722	1.79814185
22	H	0.98238600	2.32795732	-1.78765923
23	H	2.27700395	4.66624311	-1.12535946
24	H	3.66790365	4.13935352	1.18387588
25	H	2.98436322	1.40851566	4.80071451
26	H	4.50819514	2.52635252	6.41798561
27	H	6.46297979	4.98619764	5.97099186
28	H	6.73242159	3.42752755	6.85558831
29	H	7.83077957	3.89945047	5.48959164
30	H	7.04448310	3.79772696	3.15389121
31	H	5.51878708	2.69049330	1.53291027
32	H	3.83547317	-0.73038432	4.14940298
33	H	2.49570591	-3.05816725	3.57670040
34	H	1.11604734	-2.62005813	1.27165789

Table S3. Cartesian coordinates for the energy-minimized structure computed for BOD.

1	F	0.00000000	0.00000000	0.00000000
2	B	1.38454428	0.00000000	0.00000000
3	N	1.92656069	1.45989241	0.00000000
4	C	1.65913173	2.46449187	-0.87307672
5	C	0.75180865	2.37916312	-2.03201102
6	C	2.39897110	3.64193356	-0.46966986
7	C	2.37473469	4.94059805	-1.19462716
8	C	3.40733382	4.98040715	-2.32223938
9	C	3.12807103	3.31653182	0.67158598
10	C	4.03365671	4.20516133	1.42015816
11	C	2.83888326	1.93260355	0.99952054
12	C	3.27250467	1.10851492	2.04108486
13	C	4.21816852	1.65492438	3.04883661
14	C	5.60053701	1.53616816	2.84340643
15	C	6.48569452	2.05244357	3.79345335
16	C	5.99601717	2.68256617	4.94197859
17	C	4.61688463	2.79854085	5.14365944
18	C	3.72328176	2.28612275	4.19952720
19	F	1.72399759	-0.63791265	-1.18202301
20	N	1.93181203	-0.79685306	1.21975804
21	C	2.83799906	-0.21441148	2.16490714
22	C	3.12752937	-1.24284625	3.14595256
23	C	4.02263592	-1.09602979	4.30675707
24	C	2.40700285	-2.38140844	2.79042999
25	C	2.37733526	-3.69448220	3.48871347
26	C	3.39987004	-4.67148646	2.90614715
27	C	1.66983722	-2.07922492	1.58263858
28	C	0.77460992	-3.01039813	0.87185431
29	H	1.20141045	2.84604191	-2.92521676
30	H	-0.19144692	2.91879751	-1.83291671
31	H	0.46986116	1.35522447	-2.31940143
32	H	1.36000677	5.13001843	-1.60510652
33	H	2.56472887	5.77499957	-0.48520371
34	H	3.22641002	4.19209475	-3.06217823
35	H	3.38534983	5.94093856	-2.84864771
36	H	4.42372051	4.83470543	-1.93710674
37	H	4.10973437	5.20548282	0.96642568
38	H	3.70280818	4.34551433	2.46248583
39	H	5.05689509	3.79709275	1.46883006
40	H	5.98154028	1.04406378	1.94757917
41	H	7.56157031	1.96258818	3.63694008
42	H	6.69030098	3.08376338	5.68118743
43	H	4.23595804	3.29010370	6.03993360
44	H	2.64751261	2.37668283	4.35568898
45	H	5.05065857	-0.84124179	3.99976820
46	H	3.68936173	-0.29161184	4.98292532
47	H	4.08726538	-2.01767126	4.90572717

48 H	2.57331428	-3.55232733	4.57357449
49 H	1.35910048	-4.13474073	3.42931173
50 H	4.42124695	-4.28481421	3.00496648
51 H	3.35966200	-5.64042309	3.41561882
52 H	3.22429040	-4.84988448	1.83885156
53 H	1.25972168	-3.99054260	0.72244067
54 H	-0.14332829	-3.19768970	1.45725929
55 H	0.44696332	-2.66634319	-0.12025127

Table S4. Cartesian coordinates for the energy-minimized structure computed for PHEN1.

1	C	0.00000000	0.00000000	0.00000000
2	C	1.48073442	0.00000000	0.00000000
3	C	2.18958051	1.20734209	0.00000000
4	C	3.58206725	1.21032059	0.01252732
5	C	2.18991068	-1.20688929	0.00956846
6	C	3.58258845	-1.20906138	0.01894450
7	C	4.28980106	0.00070981	0.02010641
8	C	5.74548853	-0.00328012	0.03310818
9	C	6.52762139	-0.01337187	-1.07563442
10	C	6.16955026	0.17258138	-2.49575392
11	C	7.34487304	0.10543494	-3.22662824
12	C	8.42733191	-0.13998101	-2.29568528
13	N	7.94873412	-0.19596581	-1.02864087
14	B	8.73051723	-0.75026510	0.27660447
15	F	8.93934261	-2.07828276	0.19648222
16	F	9.92270995	-0.14504492	0.42017360
17	C	6.43073245	0.02772638	1.35473884
18	N	7.71658045	-0.40021048	1.54618770
19	C	8.04177828	-0.17554640	2.90201418
20	C	9.25635009	-0.48925092	3.58339193
21	C	9.54017396	0.16616734	4.80625512
22	C	10.68881905	-0.13497990	5.52127532
23	C	11.59351934	-1.09814594	5.04996969
24	C	12.82484677	-1.40630960	5.81118274
25	C	11.32005252	-1.75226863	3.84356182
26	C	10.17333694	-1.45356020	3.11751331
27	C	6.87843498	0.41237670	3.54858241
28	C	5.88093247	0.54393059	2.58262641
29	H	-0.38054806	0.01135203	1.05300693
30	H	-0.40081732	0.90216736	-0.52464371
31	H	-0.40114249	-0.91301218	-0.50526065
32	H	1.64163842	2.16243739	-0.01050463
33	H	4.12916508	2.16558566	0.01467646
34	H	1.64251116	-2.16234936	0.00741396
35	H	4.12995683	-2.16419055	0.02394654
36	H	5.15332476	0.34411664	-2.84097872
37	H	7.47590439	0.21078831	-4.30182169
38	H	9.48986103	-0.26903470	-2.53008088
39	H	8.84867330	0.93364297	5.18950012
40	H	10.89475224	0.38643714	6.46988110
41	H	13.66006672	-0.74821506	5.46011707
42	H	12.67589969	-1.22881124	6.90482821
43	H	13.13235362	-2.47074013	5.66151088
44	H	12.02061896	-2.51377751	3.46491270
45	H	9.98052919	-1.98675317	2.17249668
46	H	6.81674403	0.66555854	4.60527809
47	H	4.87238646	0.93263131	2.69600761

Table S5. Cartesian coordinates for the energy-minimized structure computed for PHEN2.

1	C	0.00000000	0.00000000	0.00000000
2	C	1.48062548	0.00000000	0.00000000
3	C	2.19122179	1.20594020	0.00000000
4	C	3.58330818	1.20572455	0.01317285
5	C	2.18902494	-1.20763805	0.01419246
6	C	3.58107989	-1.21215717	0.02391622
7	C	4.29402609	-0.00446655	0.01645985
8	C	5.74748202	0.01084942	0.04035279
9	C	6.49596347	-0.68793337	-1.03016178
10	C	5.98578127	-1.69822927	-1.92900111
11	C	7.05407168	-2.09617583	-2.72784533
12	C	8.21912147	-1.32135717	-2.32487178
13	C	9.49666611	-1.44337170	-2.94705483
14	C	9.79944843	-2.64061435	-3.64386423
15	C	11.01416795	-2.79689144	-4.29087061
16	C	11.97086213	-1.76945916	-4.27737378
17	C	13.27138634	-1.94830726	-4.95924362
18	C	11.67794839	-0.58089909	-3.59823017
19	C	10.46532610	-0.41802614	-2.94032589
20	N	7.82225940	-0.45939068	-1.27888971
21	B	8.76796091	0.51709736	-0.32314140
22	F	9.92916359	-0.09321509	-0.03154712
23	F	9.03355369	1.66611011	-0.97510812
24	C	6.45997435	0.64439340	1.01144000
25	N	7.88266571	0.79079807	1.01050740
26	C	8.24494993	1.39141310	2.18543609
27	C	9.57281697	1.73211885	2.65865407
28	C	10.57224045	2.23381457	1.81511832
29	C	11.81885287	2.58413561	2.32980959
30	C	12.09383594	2.43669229	3.69270187
31	C	13.42561684	2.79087022	4.23440489
32	C	11.09446162	1.93700036	4.53857046
33	C	9.84768439	1.59036545	4.03144953
34	C	7.05074891	1.65302241	2.98841029
35	C	5.95527804	1.22241827	2.27342223
36	H	-0.38010367	-0.01493380	1.05313293
37	H	-0.40156341	0.91436568	-0.50243038
38	H	-0.40037197	-0.90076526	-0.52751237
39	H	1.64512941	2.16225805	-0.00811142
40	H	4.13353660	2.15954095	0.02183647
41	H	1.64032115	-2.16252289	0.02004213
42	H	4.12371730	-2.17012205	0.05308208
43	H	4.95721050	-2.04811044	-1.96014632
44	H	7.04354867	-2.82642408	-3.53502222
45	H	9.06751775	-3.46413684	-3.65994218
46	H	11.23431884	-3.73687089	-4.82214257
47	H	14.00578865	-2.41567679	-4.25444893

48 H	13.16874933	-2.61699697	-5.84948550
49 H	13.68704007	-0.96659582	-5.29602691
50 H	12.41646973	0.23684279	-3.58670700
51 H	10.26027069	0.53133453	-2.41979055
52 H	10.37752258	2.35311681	0.73698349
53 H	12.59368710	2.98019778	1.65458083
54 H	14.10004446	1.89786209	4.19672773
55 H	13.89693868	3.60940486	3.63630297
56 H	13.34956096	3.12573741	5.29830430
57 H	11.29870132	1.81865317	5.61442392
58 H	9.07195705	1.19640277	4.70750514
59 H	7.07681899	2.11982086	3.97171107
60 H	4.89963849	1.25581612	2.53388963

Table S6. Cartesian coordinates for the energy-minimized structure computed for CORE.

1	F	0.00000000	0.00000000	0.00000000
2	B	1.45320577	0.00000000	0.00000000
3	F	2.03842669	1.32117097	0.00000000
4	N	1.52216206	-0.99424402	1.18395382
5	C	0.76083351	-0.86532414	2.27545205
6	C	-0.25731286	0.20705698	2.30638049
7	C	-0.99958145	0.48953658	1.10682856
8	C	-1.94028085	1.54940718	1.08308180
9	C	-2.17190184	2.33159535	2.21973034
10	C	-1.46091239	2.06659422	3.40925173
11	C	-0.52430566	1.02793662	3.44502802
12	C	1.11310134	-1.97255259	3.16301830
13	C	2.05231545	-2.79840296	2.55492708
14	C	2.66672155	-4.03516352	3.08708627
15	C	2.31182371	-2.17837433	1.22721707
16	C	2.99456581	-2.50663582	0.07264962
17	C	3.03891428	-1.75063908	-1.14358962
18	C	3.71957354	-1.83077799	-2.41926770
19	C	4.57229910	-2.92545284	-2.93182640
20	C	3.37981729	-0.62215689	-3.09046773
21	C	2.53717426	0.18028043	-2.26482614
22	C	1.97295052	1.54901537	-2.32431838
23	C	1.33298530	2.09929447	-3.47498027
24	C	0.77549518	3.38509654	-3.48134426
25	C	0.82939576	4.18044624	-2.32025516
26	C	1.44740458	3.67856387	-1.16697649
27	C	2.01743476	2.38390448	-1.15340240
28	N	2.33082684	-0.54756678	-1.13044462
29	H	-1.04909965	-0.26214704	0.20726942
30	H	-2.49546367	1.75501296	0.14923197
31	H	-2.91899421	3.14702819	2.19504747
32	H	-1.64090018	2.67860381	4.31149746
33	H	0.04235867	0.85480464	4.38078855
34	H	0.66242539	-2.12133432	4.15628723
35	H	2.31506973	-4.30808296	4.10532213
36	H	2.46494544	-4.92815814	2.45607495
37	H	3.77412841	-3.97022464	3.16463139
38	H	3.58095239	-3.45152969	0.08489954
39	H	3.99316411	-3.71186325	-3.46877484
40	H	5.34392331	-2.58992254	-3.66022756
41	H	5.13838302	-3.47390181	-2.14701499
42	H	3.74178626	-0.32955387	-4.08884642
43	H	1.25585788	1.48837159	-4.39629640
44	H	0.29101730	3.77292025	-4.39618415
45	H	0.39629124	5.19824885	-2.32396019
46	H	1.49109134	4.29837692	-0.25197622
47	H	2.71271043	2.15099271	-0.23188535

Table S7. Effect of temperature on the nonradiative rate constant. The rate constants are expressed in units of 10^9 s^{-1} .

Temperature / K	CORE	BOD	PHEN2	ROBOD	PHEN1
140	0.0085	0.0195	0.0015	0.022	0.030
150	0.0120	0.0210	0.0170	0.065	0.12
160	0.0107	0.0190	0.0480	0.174	0.35
170	0.0100	0.0170	0.0850	0.395	0.71
180	0.0100	0.0175	0.1060	0.616	1.20
190	0.0130	0.0170	0.1315	1.116	1.71
200	0.0140	0.0170	0.1335	1.438	2.43
210	0.0120	0.0185	0.1560	1.806	3.18
220	0.0120	0.0230	0.1610	2.20	4.00
230	0.0140	0.0210	0.2000	2.75	4.90
240	0.0096	0.0230	0.2080	3.22	6.28
250	0.0115	0.0245	0.2360	4.03	7.10
260	0.0125	0.0305	0.2630	4.19	8.37
270	0.0130	0.0370	0.2860	5.08	9.60
280	0.0090	0.0460	0.3335	6.34	10.10
290	0.0120	0.0520	0.3430	6.50	10.73

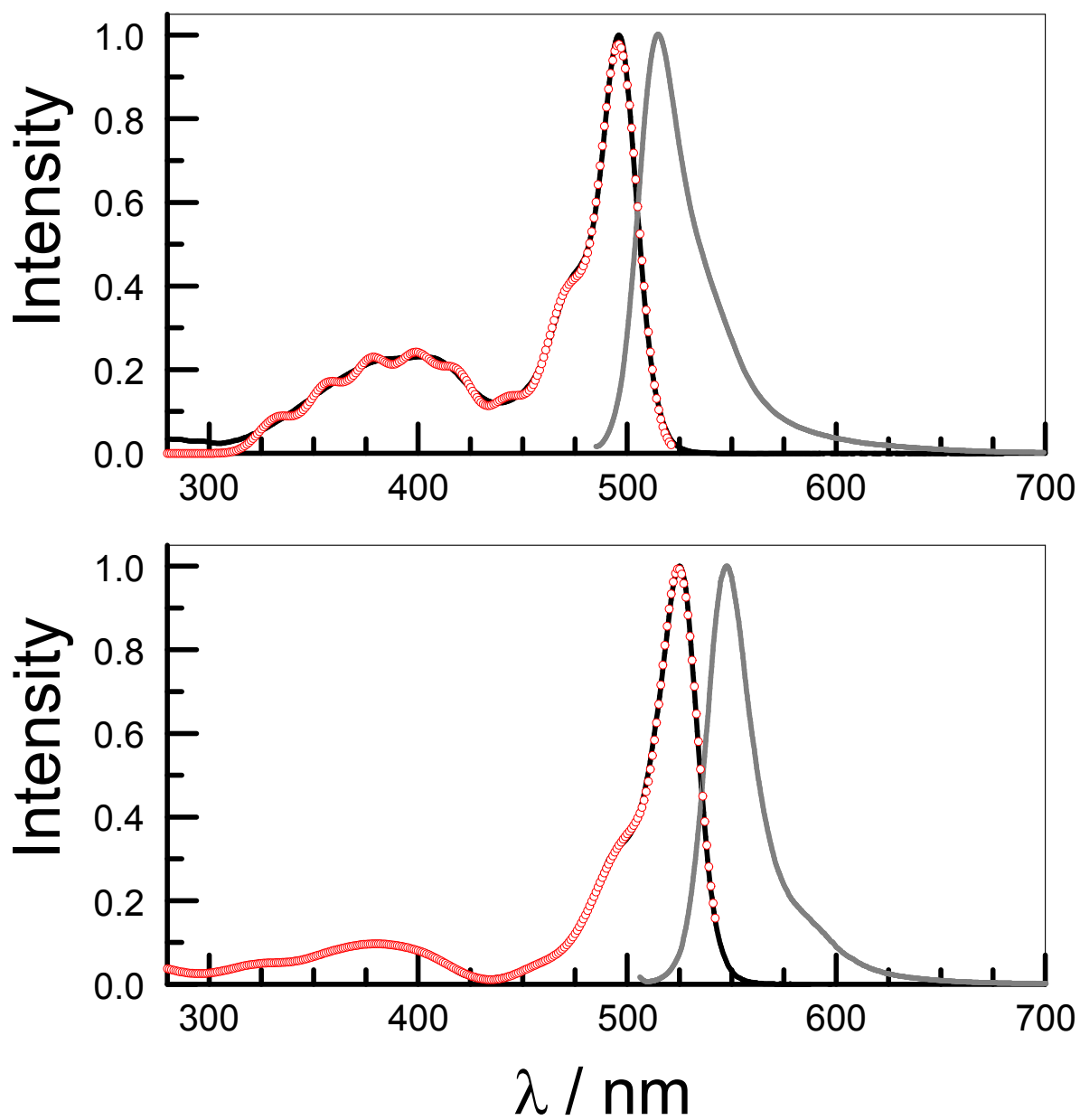
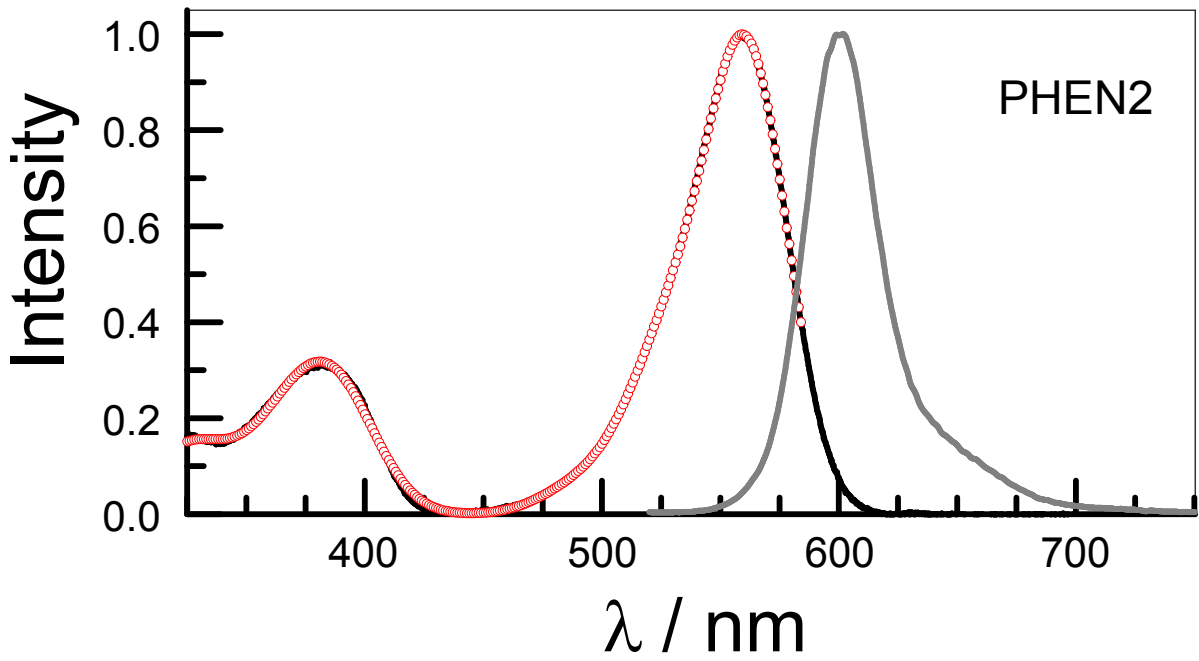
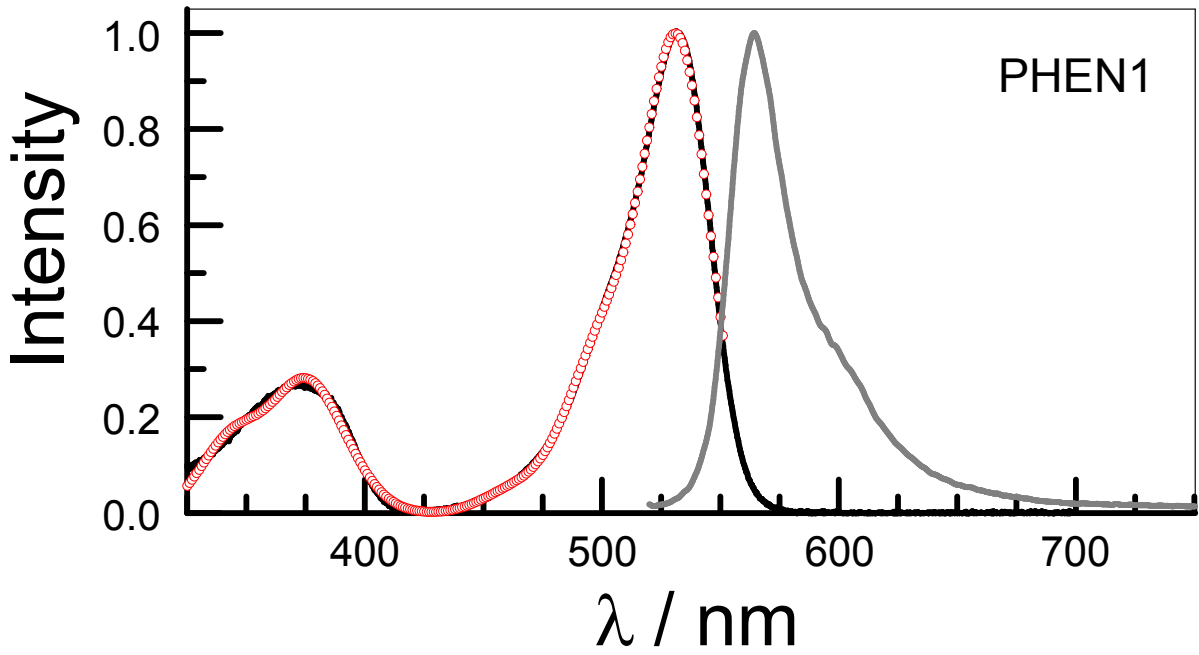


Figure S1. Comparison of absorption (black curve), fluorescence (grey curve) and excitation (red circles) spectra recorded for ROBOD (upper panel) and BOD (lower panel) in MTHF at room temperature.



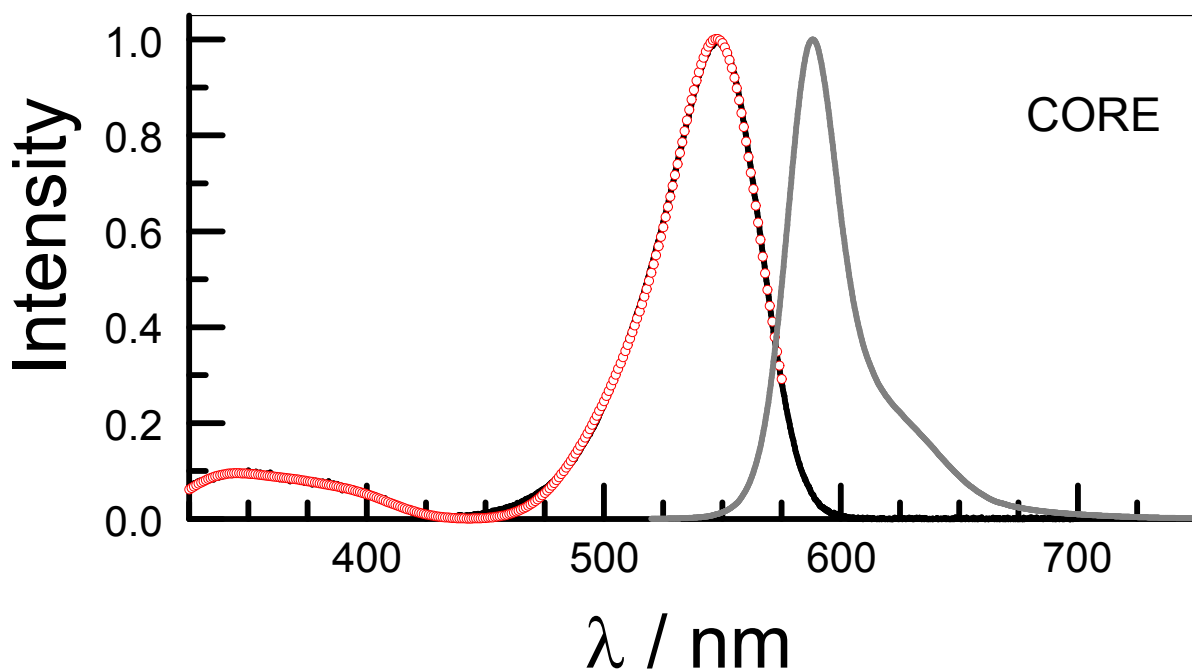


Figure S2. Comparison of absorption (black curve), fluorescence (grey curve) and excitation (red circles) spectra recorded for the Bodipy-based dyes in MTHF at room temperature.

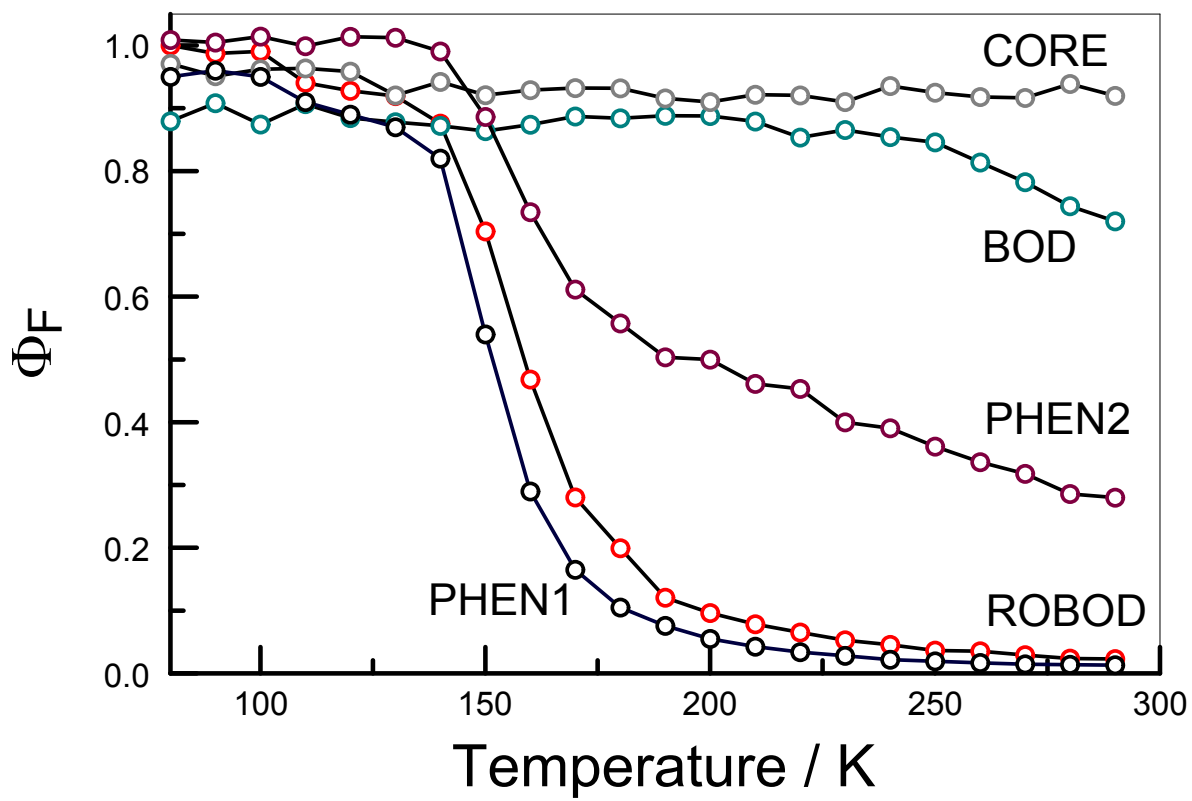


Figure S3. Effect of temperature on the emission quantum yield measured for the various Bodipy-based dyes in MTHF solution.

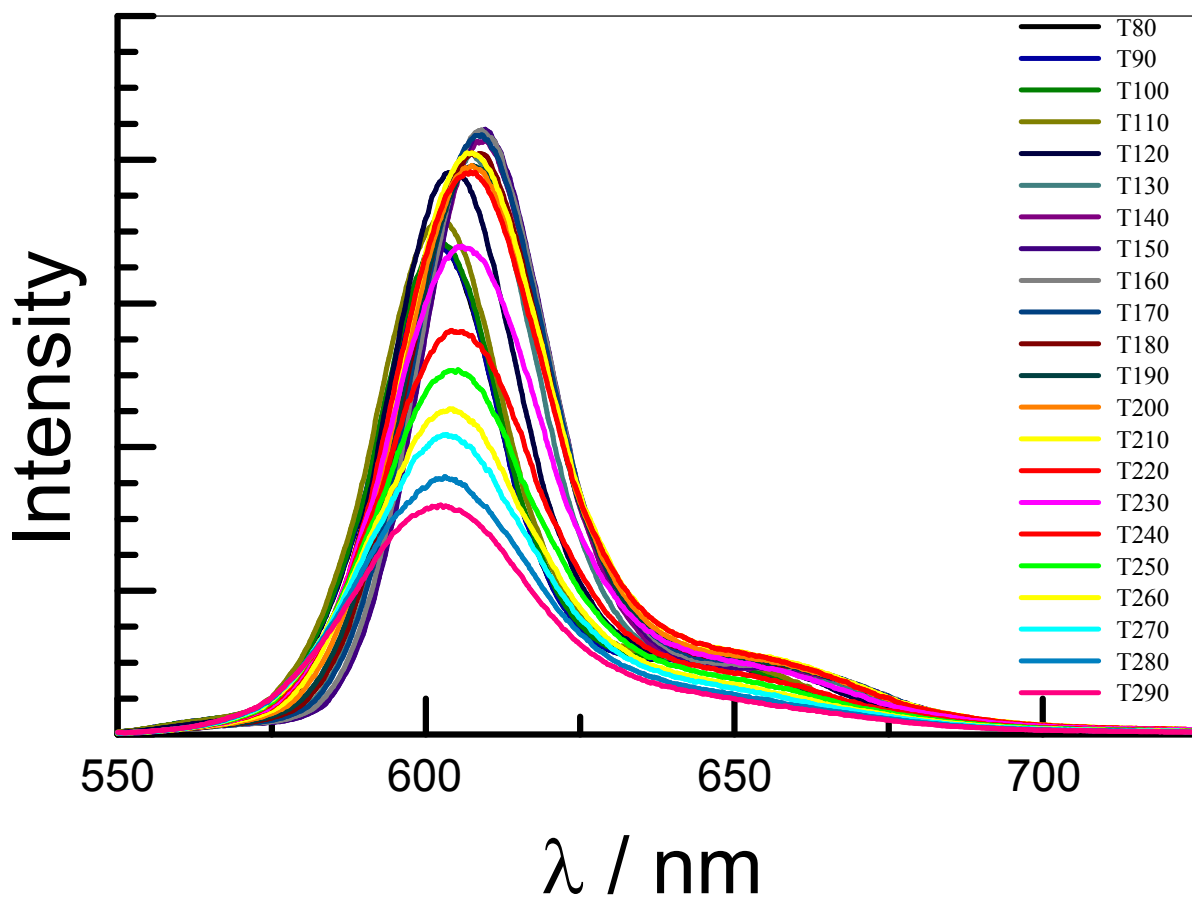


Figure S4. Effect of temperature on the fluorescence spectral profile recorded for PHEN2 in MTHF.

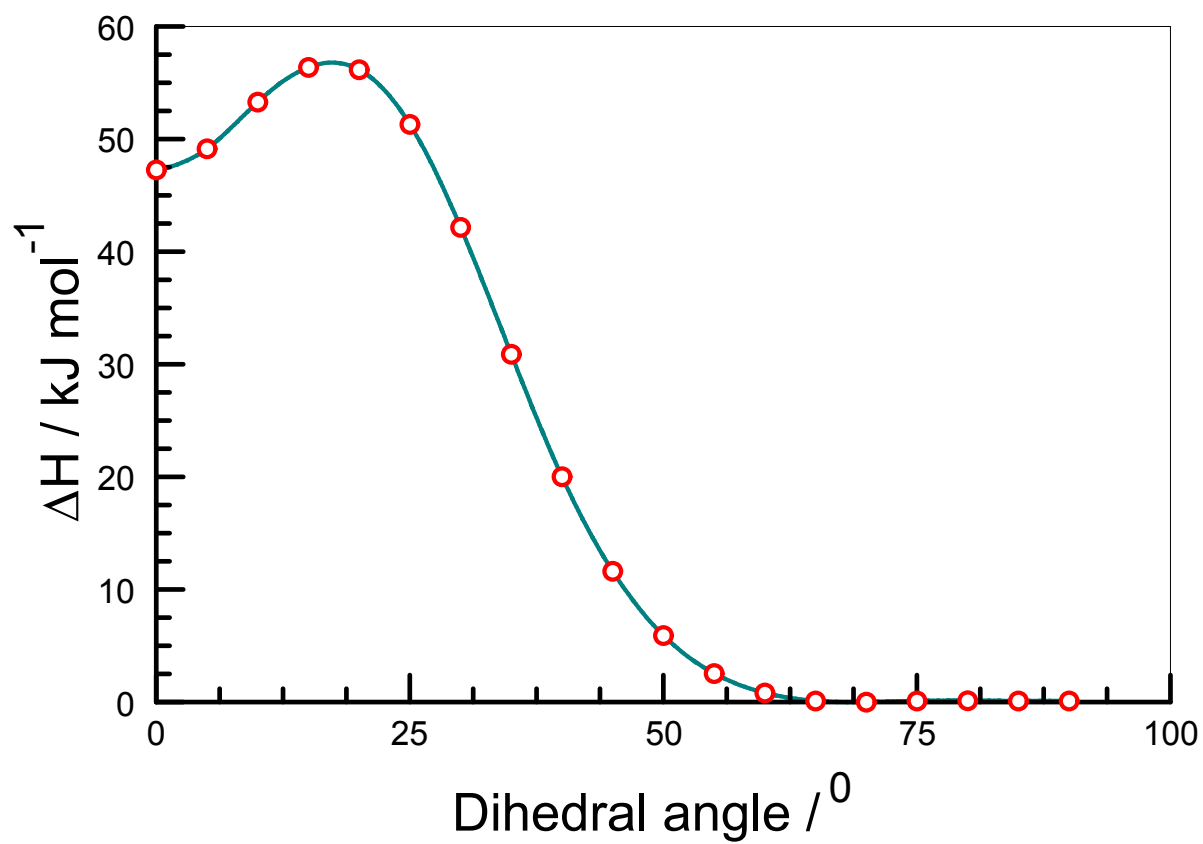


Figure S5. Effect of dihedral angle between the dipyrin nucleus and the 2-tolyl ring on the total enthalpy of the molecule as computed for PHEN1 in a solvent reservoir.

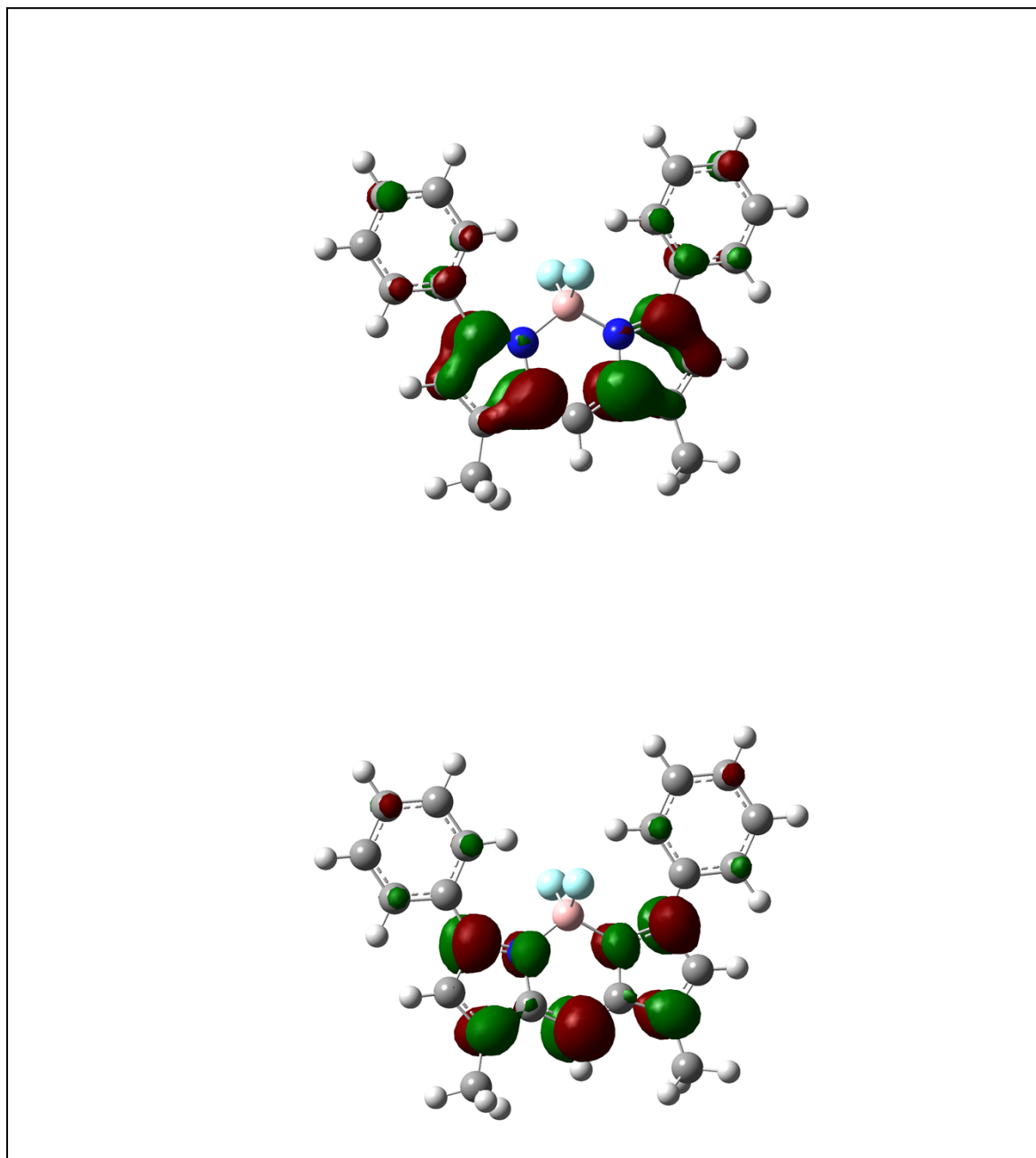


Figure S6a. Kohn-Sham representations of the HOMO (upper panel) and LUMO (lower panel) isodensity ($id = 0.02$) distributions computed for CORE with the 3,5-aryl rings held at a co-planar geometry.

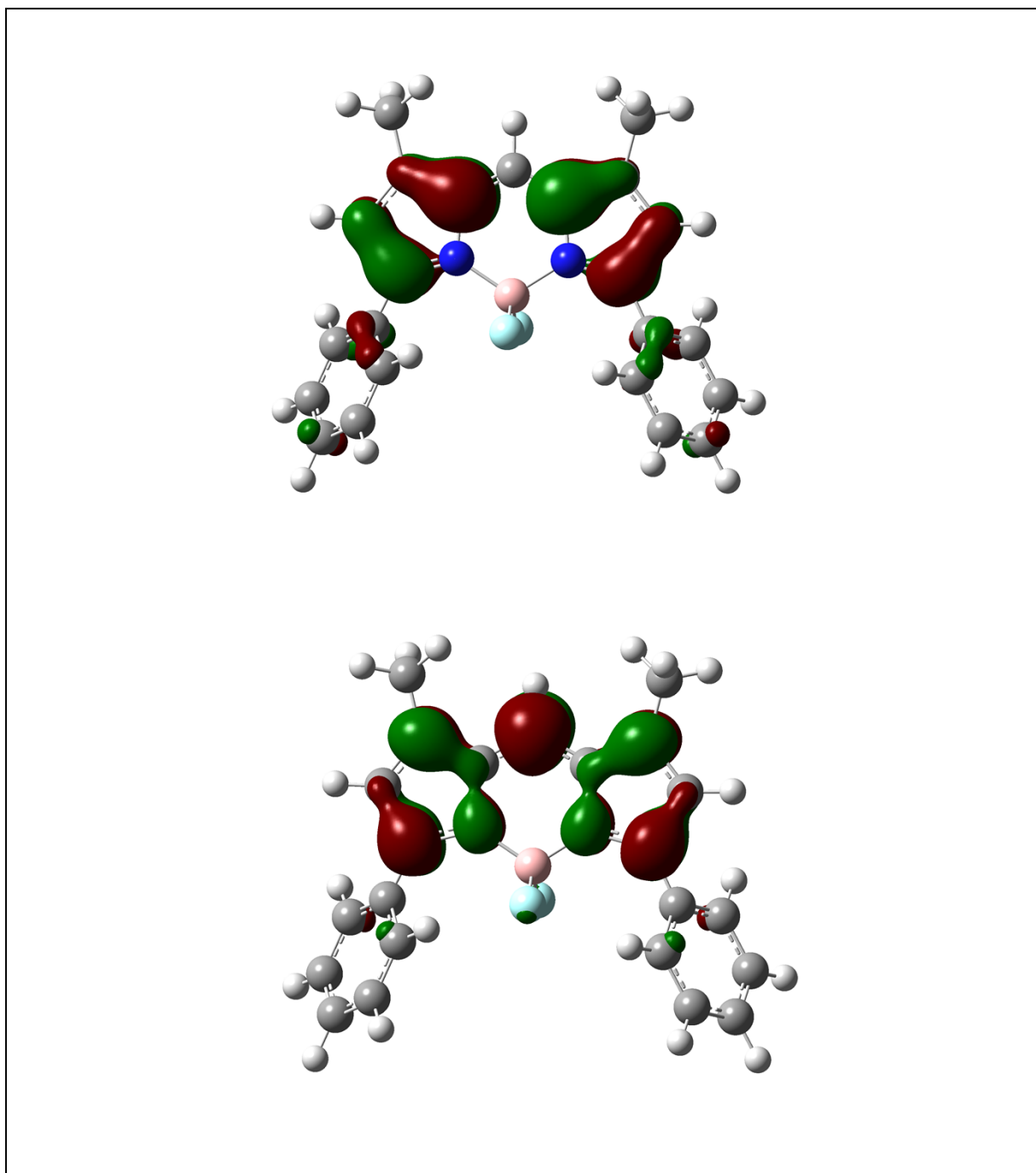


Figure S6b. Kohn-Sham representations of the HOMO (upper panel) and LUMO (lower panel) isodensity ($\text{id} = 0.017$) distributions computed for CORE with the 3,5-aryl rings held at the optimized geometry.

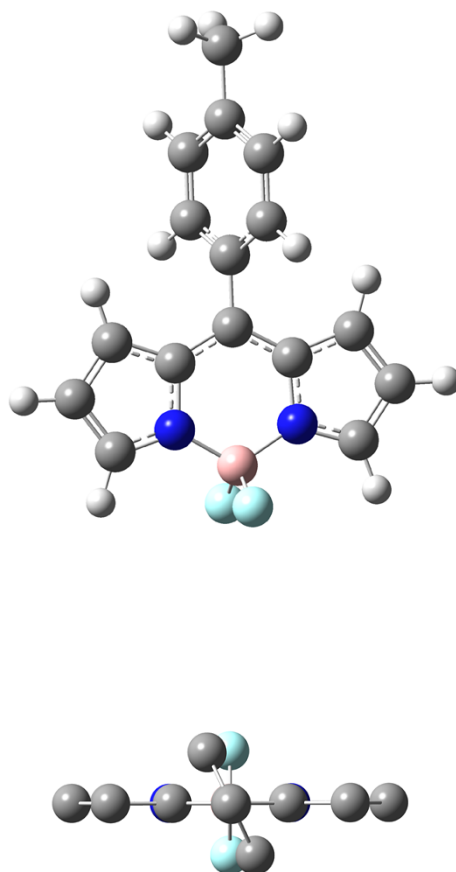


Figure S7a. Energy-minimized geometry computed for ROBOD (upper panel). The lower panel shows a projection looking from the methyl carbon atom of the meso-tolyl group down to the boron atom.

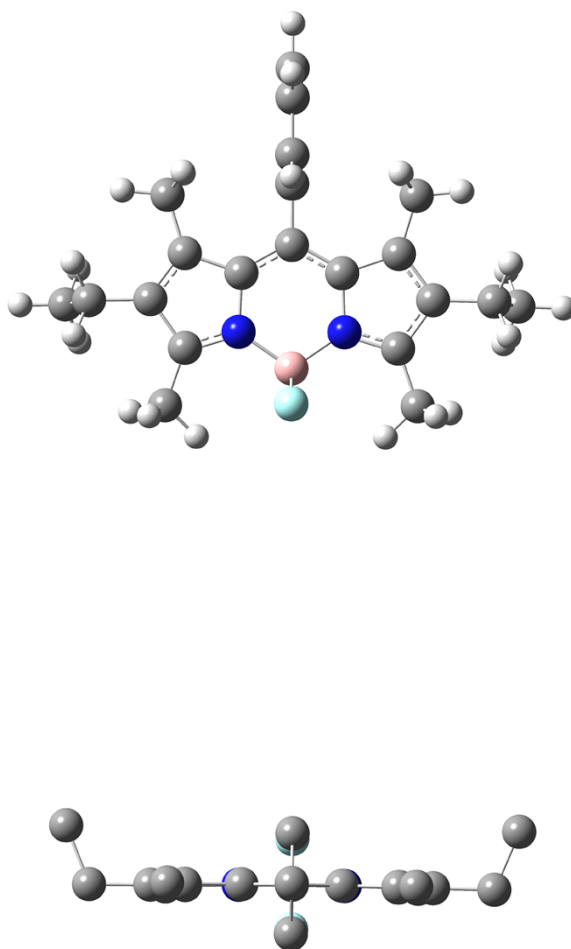


Figure S7b. Energy-minimized geometry computed for BOD (upper panel). The lower panel shows a projection looking from the para carbon atom of the meso-phenyl group down to the boron atom.

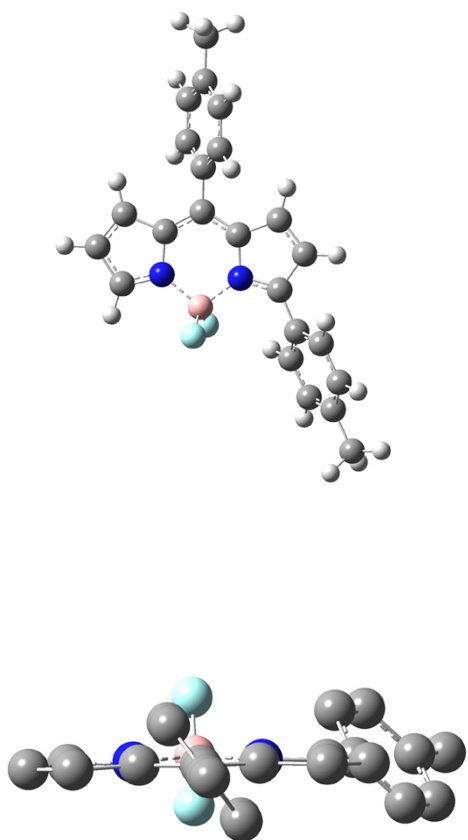


Figure S7c. Energy-minimized geometry computed for PHEN1 (upper panel). The lower panel shows a projection looking from the methyl carbon atom of the meso-tolyl group down to the boron atom.

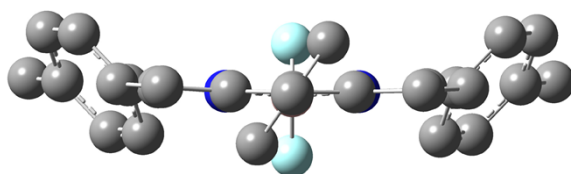
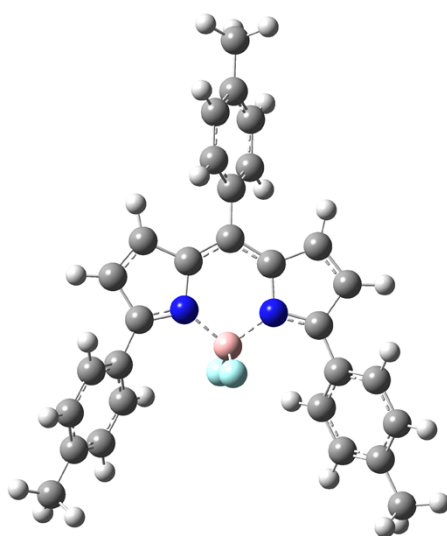


Figure S7d. Energy-minimized geometry computed for PHEN2 (upper panel). The lower panel shows a projection looking from the methyl carbon atom of the meso-tolyl group down to the boron atom.

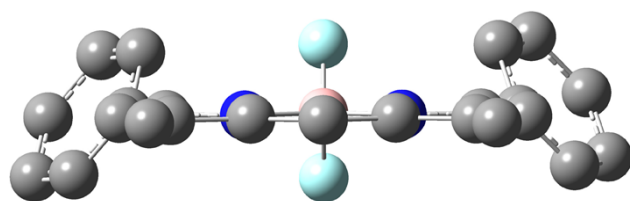
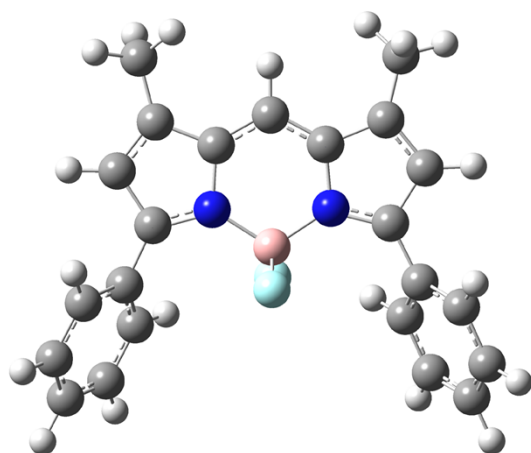


Figure S7e. Energy-minimized geometry computed for CORE (upper panel). The lower panel shows a projection looking from the methyl carbon atom of the meso-tolyl group down to the boron atom.

EXPERIMENTAL DETAILS

General methods for the synthesis and NMR characterization.

When needed, reactions were performed under a dry atmosphere of argon using standard Schlenk tube techniques. CH_2Cl_2 was distilled from P_2O_5 under an argon atmosphere. CHCl_3 was neutralized on basic alumina prior to use. Et_2O and THF were distilled over sodium/benzophenone under an argon atmosphere. Toluene was distilled from sodium under an argon atmosphere. Triethylamine was distilled over KOH. Elementary magnesium was treated with 1M HCl, washed with water and intensively dried prior to use. ^1H NMR, ^{13}C NMR and ^{11}B NMR spectra were recorded on BRUCKER Spectrometers and chemical shifts were reported to the delta scale in ppm relative to the residual peak of the deuterated used solvent: CHCl_3 ($\delta = 7.26$ ppm) or CDHCl_2 ($\delta = 5.32$ ppm) for ^1H NMR, relative to CDCl_3 ($\delta = 77.16$ ppm) or CD_2Cl_2 ($\delta = 54.00$ ppm) for ^{13}C NMR and were calibrated with the borosilicate of the NMR tubes for ^{11}B NMR.

General procedure for the Suzuki cross-coupling reaction. A Schlenk tube was charged with a solution of appropriate iodo- and aryl- boronic acid or boronate derivatives in toluene. A mineral base (K_2CO_3 or Cs_2CO_3) was also added. The solution was degassed with argon for 30 minutes, then $[\text{Pd}(\text{PPh}_4)_3]$ was added. The mixture was stirred at 60°C until complete consumption of the starting material (monitored by TLC). The solution was then extracted with toluene, washed with water, dried over MgSO_4 and evaporated under vacuum. The residue was purified by column chromatography.

PHEN1. This compound was prepared according to the general procedure using 8-tolyl-3-bromo-BODIPY (167.0 mg, 0.462 mmol) in toluene (10 mL), *p*-tolylboronic acid (0.554 mmol, 75.0 mg), aqueous K_2CO_3 (2.31 mmol, 319.0 mg), at 110°C during 15 min. The product was purified using a chromatography column packed with flash silica gel, using petroleum ether/ CH_2Cl_2 (6:4) as eluant. The pure product was recovered as a purple powder (100.0 mg, 58%). ^1H NMR (200 MHz, CDCl_3): δ (ppm) = 7.79 (m, 1H), 7.57 (ABsyst., 4H, $J_{\text{AB}} = 5.0$ Hz, $\nu_0\delta = 117.3$ Hz), 7.38 (ABsyst., 4H, $J_{\text{AB}} = 7.9$ Hz, $\nu_0\delta = 28.1$ Hz), 7.79 (d, 1H, $^3J = 4.4$ Hz), 6.83 (d, 1H, $^3J = 4.0$ Hz), 6.66 (d, 1H, $^3J = 4.4$ Hz), 6.50-6.47 (m, 1H), 2.46 (s, 3H), 2.47 (s, 3H). ^{13}C NMR (75 MHz, $(\text{CD}_3)_2\text{CO}$) δ (ppm) = 161.4, 146.5, 142.5, 141.9, 141.2, 138.0, 134.7, 133.9, 132.1, 131.6, 130.5, 130.4, 130.4, 130.3, 130.1, 129.9, 122.0, 118.8, 21.4. ^{11}B NMR (128 MHz, CDCl_3) δ (ppm) = 0.86 (t, $^1J = 94$ Hz). UV-Vis (CH_2Cl_2) λ

nm (ϵ , $M^{-1}\cdot\text{cm}^{-1}$): 531 (59000) ; 370 (16000). EI, m/z (%): 372.1 (100). Anal. Calcd for $C_{23}H_{19}BF_2N_2$: C, 74.22; H, 5.15; N, 7.53. Found: C, 74.04; H, 4.89; N, 7.84.

PHEN2. This compound was prepared according to the general procedure from 8-tolyl-3,5-dibromoBODIPY (200.0 mg, 0.455 mmol) in toluene (15 mL), *p*-tolylboronic acid (0.955 mmol, 129.8 mg), aqueous K_2CO_3 (2.27 mmol, 314.2mg), at 110°C during 1h. The product was purified using a chromatography column packed with flash silica gel, using petroleum ether / CH_2Cl_2 (7:3 to 6:4) as eluant. The pure product was recovered as a purple powder (151.6 mg, 72%). 1H NMR (200 MHz, $CDCl_3$): δ (ppm) = 7.70 (ABsyst., 8H, J_{AB} = 8.2 Hz, $\nu_0\delta$ = 166.7 Hz), 7.41 (ABsyst., 4H, J_{AB} = 8.1 Hz, $\nu_0\delta$ = 45.2 Hz), 6.89 (d, 2H, 3J = 4.4 Hz), 6.61 (d, 2H, 3J = 4.4 Hz), 2.48 (s, 3H), 2.39 (s, 6H). ^{13}C NMR (75 MHz, $CDCl_3$): δ (ppm) = 158.7, 143.7, 140.4, 139.6, 136.3, 131.7, 130.6, 129.9, 129.4, 129.4, 129.0, 128.9, 120.6, 21.5. ^{11}B NMR (128 MHz, $CDCl_3$) δ (ppm) = 1.49 (t, 1J = 100 Hz). EI, m/z (%): 462.1 (100). Anal. Calcd for $C_{30}H_{25}BF_2N_2$: C, 77.93; H, 54.45; N, 6.06. Found: C, 77.82; H, 5.26; N, 5.75.

CORE. To a degassed solution of 4-methyl-2-phenyl-*1H*-pyrrole (373.7 mg, 2.38 mmol, 2 equiv) in CH_2Cl_2 (30 mL) were successively added triethyl orthoformate (3 mL, 18.04 mmol, 15 equiv) and trifluoroacetic acid (0.55 mL, 7.19 mmol, 6 equiv). The solution was stirred at rt for 4h, then was concentrated and the excess of triethyl orthoformate was removed under vacuum. The purple residue was solubilized in CH_2Cl_2 (30 mL) under argon, iPr_2NH (1 mL, 7.14 mmol, 6 equiv) was first added, giving a pink solution; then $BF_3\cdot OEt_2$ (1.17 mL, 9.48 mmol, 8 equiv) was finally added. The purple solution was stirred at room temperature for 16 h, then poured into a saturated solution of $NaHCO_3$ and stirred further for 2 h. The reaction medium was washed with H_2O , dried with brine and over Na_2SO_4 . Purification by column chromatography (SiO_2 , CH_2Cl_2 /petroleum ether (gradient from 50/50 to 100/0), then crystallization from CH_2Cl_2 /EtOH gave dark green metallic needles (308.6 mg, 70%). 1H NMR, 400 MHz, CD_2Cl_2 , δ (ppm): 2.39 (s, 6H); 6.47 (s, 2H); 7.39 (s, 1H); 7.42-7.45 (m, 6H); 7.82-7.84 (m, 4H). ^{13}C NMR, 100 MHz, CD_2Cl_2 , δ (ppm): 11.1; 120.5; 122.0; 128.1; 129.3 (t, J_{C-F} = 3.9 Hz); 129.4; 132.7; 135.3; 141.9; 157.8. ^{11}B NMR, 128 MHz, CD_2Cl_2 , δ (ppm): 1.33 (t, 1B, J = 32.1Hz). IR: (cm^{-1}): 3096; 3039; 2924; 1607; 1592; 1515; 1489; 1454; 1393; 1220; 1192; 1150; 1031; 994; 952; 807; 764; 725; 694; 679. Mp = 217.1-217.5 °C. EI (m/z , relative intensity): theoretical mass 372.2 (100), 373.2 (25.6); found 372.1 (100). Anal. calcd for $C_{23}H_{19}BF_2N_2$ (M_r = 372.22): C, 74.22; H, 5.15; N, 7.53. Anal. found: C, 74.14; H, 5.09; N, 7.47.

Spectroscopic investigations.

Absorption spectra were recorded with a Hitachi U3310 spectrophotometer and luminescence spectra were recorded with a fully-corrected Jobin-Yvon Fluorolog tau-3 spectrophotometer. Emission spectra were recorded for optically dilute solutions after purging with N₂. Luminescence quantum yields were determined^{S1} relative to Cresyl Violet ($\Phi_F = 0.54$)^{S2} in methanol, fluorescein ($\Phi_F = 0.95$)^{S3} in 0.1M NaOH or Nile Blue ($\Phi_F = 0.27$)^{S4} in ethanol. Emission lifetimes were measured at room temperature by time-correlated, single photon counting using a picosecond laser diode (fwhm = 60 ps) as excitation source. Emission was isolated from scattered laser light with a narrow bandpass filter and detected with a microchannel plate photocell. After deconvolution of the instrument response function, the time resolution of this set-up was *ca.* 40 ps. Temperature dependence studies were made with an Oxford Instruments Optistat DN. All samples were purged thoroughly with N₂ before being sealed into optical cuvettes. Corrections for contraction of the solvent were made on the basis of literature precedents.^{S5}

Quantum chemical calculations

Semi-empirical calculations were performed with the PM6 parameterization^{S6} within in the framework of the AMPAC^{S7} 10.1 program package. Calculations were made for energy-minimized structures at the restricted Hartree-Fock (RHF) level with the solute embedded in a solvent reservoir of dielectric constant 10 using the COSMO^{S8} model. Stationary points on the reaction potential energy surface were determined without geometrical constraints using the FULLCHN protocol to obtain first approximations. Further refinement was achieved using the eigenvector following procedure. All stationary points were verified as being genuine transition states by calculation of vibrational frequencies. Rotational barriers were computed by systematic variation of the respective dihedral angles from those of the energy-minimized structures with single-point (PM6, RHF, COMO) calculation of the energy. This approach assumes a rigid geometry for the dipyrin backbone. Refined calculations were made using FULLCHN where the entire molecule was allowed to undergo structural deformation in order to accommodate full rotation of the *meso*-aryl ring.

The *ab initio* calculations were carried out with the Gaussian 09^{S9} program package. For the DFT calculations, Becke's three-parameter (B3) gradient-corrected exchange functional^{S10} combined with the Lee-Yang-Parr (LYP) correlation functional^{S11} was used.

Ground-state structures were computed with the RHF method used in conjunction with the 6-31G** basis set and with the PCM model^{S12} for the surrounding solvent reservoir. The geometries of the relevant excited states were optimized by the restricted single-excited configuration interaction approach (CIS) within the Hartree-Fock (HF) approximation.^{S13}

References

- S1. A. M. Brouwer, Standards for photoluminescence quantum yield measurements in solution. *Pure Appl. Chem.* **2011**, *83*, 2213-2228.
- S2. D. Magde, J. H. Brannon, T. L. Cremers and J. Olmsted III, Absolute luminescence yield of Cresyl Violet. A standard for the red. *J. Phys. Chem.* **1979**, *83*, 696-699.
- S3. J. H. Brannon and D. Magde, Absolute quantum yield determination by thermal blooming. Fluorescein. *J. Phys. Chem.* **1978**, *82*, 705-709.
- S4. R. Sens and K. H. Drexhage, Fluorescence quantum yields of Oxazine and Carbazine laser dyes. *J. Lumin.* **1981**, *24-25*, 709-712.
- S5. P. D. Zoon and A. M. Brouwer, A Push-Pull Aromatic Chromophore with a touch of merocyanine. *Photochem. Photobiol. Sci.* **2009**, *8*, 345-353.
- S6. J. J. P. Stewart, Optimization of parameters for semi-empirical methods. V: Modification of NDDO approximations and applications to 70 elements. *J. Mol. Model.* **2007**, *13*, 1173-1213.
- S7. **AMPAC 10**, 1992-2013 Semichem, Inc. 12456 W 62nd Terrace - Suite D, Shawnee, KS 66216.
- S8. A. Klamt, Calculation of UV/Vis spectra in solution. *J. Phys. Chem.* **1996**, *100*, 3349-3353.
- S9. Gaussian 09, Revision D.01, M. J. Frisch, G. W. Trucks, H. B. Schlegel, G. E. Scuseria, M. A. Robb, J. R. Cheeseman, G. Scalmani, V. Barone, B. Mennucci, G. A. Petersson, H. Nakatsuji, M. Caricato, X. Li, H. P. Hratchian, A. F. Izmaylov, J. Bloino, G. Zheng, J. L. Sonnenberg, M. Hada, M. Ehara, K. Toyota, R. Fukuda, J. Hasegawa, M. Ishida, T. Nakajima, Y. Honda, O. Kitao, H. Nakai, T. Vreven, J. A. Montgomery Jr., J. E. Peralta, F. Ogliaro, M. Bearpark, J. J. Heyd, E. Brothers, K. N. Kudin, V. N. Staroverov, R. Kobayashi, J. Normand, K. Raghavachari, A. Rendell, J. C. Burant, S. S. Iyengar, J. Tomasi, M. Cossi, N. Rega, N. J. Millam, M. Klene, J. E. Knox, J. B. Cross,

- V. Bakken, C. Adamo, J. Jaramillo, R. Gomperts, R. E. Stratmann, O. Yazyev, A. J. Austin, R. Cammi, C. Pomelli, J. W. Ochterski, R. L. Martin, K. Morokuma, V. G. Zakrzewski, G. A. Voth, P. Salvador, J. J. Dannenberg, S. Dapprich, A. D. Daniels, Ö. Farkas, J. B. Foresman, J. V. Ortiz, J. Cioslowski and D. J. Fox, Gaussian, Inc., Wallingford CT, 2009.
- S10. A. D. Becke, Density functional thermochemistry. III The role of exact exchange. *J. Chem. Phys.* **1993**, *98*, 5648-5652.
- S11. C. Lee, W. Yang and R. G. Parr, Development of the Colle-Salvetti correlation energy formula into a functional of the electron density. *Phys. Rev. B* **1988**, *37*, 785-789.
- S12. B. Mennucci, C. Cappelli, C. A. Guido, R. Cammi and J. Tomasi, Structures and properties of electronically excited state chromophores in solution from the Polarizable Continuum Model coupled to the TD-DFT. *J. Phys. Chem. A* **2009**, *113*, 3009-3200.
- S13. J. B. Foresman, M. Head-Gordon, J. A. Pople and M. J. Frish, Toward a systematic molecular orbital theory for excited states. *J. Phys. Chem.* **1992**, *96*, 135.